4-15-1993

Dynamical low-energy electron-diffraction investigation of lateral displacements in the topmost layer of Pd(110)

O. L. Warren
Iowa State University

Patricia A. Thiel
Iowa State University, thiel@ameslab.gov

Dynamical low-energy electron-diffraction investigation of lateral displacements in the topmost layer of Pd(110)

Abstract
Based on He-atom diffraction evidence for an order-disorder transition on Pd(110) at 230 K, other authors have proposed a model in which the atoms of the topmost layer are displaced laterally by 0.7 Å along the [001] direction, with the directions of the displacements correlated at T<230 >K, but largely uncorrelated at T>230 K. To test this model, we have examined the proposed ordered phase by dynamical low-energy electron-diffraction analysis. Our results favor a nonlaterally displaced geometry, with a contraction of 4.4±1.5% in the first interlayer spacing and an expansion of 1.5±1.5% in the second interlayer spacing, but do not conclusively rule out the possibility of lateral displacements

Keywords
Ames Laboratory

Disciplines
Physical Chemistry

Comments
This article is from *Physical Review B* 47, no. 16 (1993): 10848–10851, doi:10.1103/PhysRevB.47.10848.

Dynamical low-energy electron-diffraction investigation of lateral displacements in the topmost layer of Pd(110)

O. L. Warren and P. A. Thiel
Department of Chemistry and Ames Laboratory, Iowa State University, Ames, Iowa 50011
(Received 2 September 1992)

Based on He-atom diffraction evidence for an order-disorder transition on Pd(110) at 230 K, other authors have proposed a model in which the atoms of the topmost layer are displaced laterally by 0.7 Å along the [001] direction, with the directions of the displacements correlated at $T<230$ K, but largely uncorrelated at $T>230$ K. To test this model, we have examined the proposed ordered phase by dynamical low-energy electron-diffraction analysis. Our results favor a nonlaterally displaced geometry, with a contraction of $4.4\pm1.5\%$ in the first interlayer spacing and an expansion of $1.5\pm1.5\%$ in the second interlayer spacing, but do not conclusively rule out the possibility of lateral displacements $<$ca. 0.13 Å. Nevertheless, lateral displacements of the magnitude required to account for the He-atom diffraction results are clearly not present.

I. INTRODUCTION

The unreconstructed surface of clean Pd(110) has been the subject of numerous conflicting studies. In a He-atom diffraction study restricted to angular scans along the [001] direction, Francis and Richardson[1] observed substantial evidence for an order-disorder transition—possibly first order—on Pd(110) at 230 K, where the average domain width along the [001] direction exceeded the limit set by an instrumental transfer width of 50 Å at $T<230$ K, but was limited to only about 2–3 unit cells at $T>230$ K. Since Francis and Richardson were able to rule out the formation of small islands or narrow terraces, they proposed that the atoms of the topmost layer were displaced laterally along the [001] direction, where the directions of the displacements were correlated at $T<230$ K, but largely uncorrelated at $T>230$ K. An analysis of the diffraction profiles yielded an estimate of 0.7 Å for the magnitude of the displacements. Subsequently, in a study of low-energy electron-diffraction (LEED) profiles, Wolf *et al.*[2] observed subtle evidence for an order-disorder transition on Pd(110) at 250 K; however, in contrast to the results of Francis and Richardson, their results indicated that better order existed along the [001] direction at $T>250$ K. An analysis of the LEED profiles yielded an average domain width of 20 unit cells along the [001] direction at $T<250$ K and an average domain width of 28 unit cells along the [001] direction at $T>250$ K. Wolf *et al.* attributed the differences in the two studies to either different surface conditions or differences in the way electrons and He atoms probe the surface. Recently, Guillopé and Legrand[3] presented theoretical support for the existence of an order-disorder transition on Pd(110) at low temperature; however, they favored a transition between a nonlaterally displaced phase at low temperature and a laterally disordered phase at higher temperature. Finally, Lahee, Toennies, and Wöll[4] attempted to reproduce the results of Francis and Richardson in a subsequent He-atom diffraction study, but found no evidence for an order-disorder transition on Pd(110). Since each of the results mentioned above pertain to the surface geometry of Pd(110), we conclude that there is no consensus in this regard.

If an order-disorder transition does occur on Pd(110) near 250 K, its effect on LEED intensity-energy [$I(E)$] curves appears to be negligible. In the initial dynamical LEED study, Diehl *et al.*[5] varied the first two interlayer spacings in an analysis of $I(E)$ curves collected at 300 K, and obtained a contraction of $5.7\pm2\%$ in the first interlayer spacing and an expansion of $0.5\pm2\%$ in the second interlayer spacing. Subsequently, Skottke *et al.*[6] varied the first two interlayer spacings in an analysis of $I(E)$ curves collected at 130 K, and obtained a contraction of $5.1\pm1.5\%$ in the first interlayer spacing and an expansion of $2.9\pm1.5\%$ in the second interlayer spacing. Although both analyses were carried out for an assumed nonlaterally displaced geometry, we believe that the close similarity between the interlayer spacings obtained above and below the proposed transition temperature favors either the absence of a phase transition or favors a phase transition in which the local geometry remains the same in both phases—such as has been proposed by Francis and Richardson.

In this report, we present the results of a quantitative test of the model proposed by Francis and Richardson by dynamical LEED analysis. In agreement with previous dynamical LEED results, we find that $I(E)$ curves collected above and below the proposed transition temperature do not differ significantly; thus we have restricted our analysis to curves collected below the proposed transition temperature. We assume that the surface is ordered; therefore our incorporation of lateral displacements entails a rigid shift of the topmost layer along the [001] direction.

II. EXPERIMENTAL PROCEDURES

Experiments are performed in a stainless-steel ultrahigh-vacuum chamber (base pressure $\leq 1\times10^{-10}$ torr) equipped with a single-pass cylindrical mirror analyzer for Auger electron spectroscopy (AES); μ-metal shielded, display type, four-grid LEED optics; quadru-

pole mass spectrometer; sputter gun; and provisions for gas exposure. The Pd(110) crystal is cleaned by cycles of Ar^+ bombardment at 300 K and annealing at 1100 K until impurity concentrations, with the exception of carbon, are reduced to the noise level of AES. Due to the overlap of the carbon 272-eV and Pd 279-eV Auger transitions, additional steps are taken to ensure that carbon levels are sufficiently low. Oxygen exposure at 640 K to remove carbon as carbon oxides and flashes to 1100 K to desorb residual oxygen are performed until the ratio of Pd 279-eV to Pd 330-eV AES peak-to-peak heights is reduced to a limiting value of ca. 0.17 (2-keV primary beam energy and 1-V peak-to-peak modulation voltage are used for AES work). After cleaning in this manner, the surface exhibits a high-quality (1×1) LEED pattern. As a test to see if surface saturation can be achieved upon gas exposure, the (2×1) $p1g1$ LEED pattern of the CO-saturated surface[7] and the (1×2) LEED pattern of the hydrogen-induced paired-row reconstruction[8] are reproduced. Thermal desorption spectra from the CO-saturated surface are regularly consistent with those previously reported for a carbon-free surface.[9]

Nineteen normal-incidence $I(E)$ curves are acquired simultaneously (45–250 eV, 1-eV grid) in ca. 10 min with a computer-interfaced video processor and a silicon-intensified-target camera. The crystal is maintained at 105 K during data collection. Normal incidence is determined by comparing symmetry-equivalent curves. The ability to achieve normal incidence is demonstrated in Fig. 1. Sixteen video frames are averaged at each energy to improve the signal-to-noise ratio. Camera saturation effects are tested by acquiring curves over a wide range of camera aperture settings. Background subtraction is performed locally during data acquisition. Beam current normalization is performed separately by measuring the current as a function of beam energy with the crystal biased sufficiently positive to suppress secondary emission. Equivalent beam averaging (a procedure known to minimize residual experimental errors[10]) is performed when possible, which reduces the set of 19 curves to 8 symmetry-nonequivalent curves over a total-energy range of $\Delta E = 1153$ eV. Beam indices are as follows: (0,1), (1,0), (1,1), (0,2), (2,0), (1,2), (2,1), and (0,3). Curves collected in two separate experiments are in excellent agreement, and are averaged to further enhance statistical reliability.

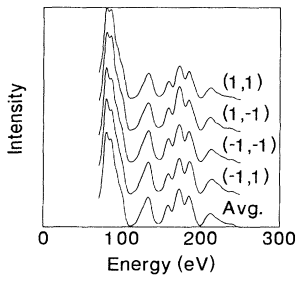

FIG. 1. Comparison between experimental $I(E)$ curves for the (1,1) beam set and their average at normal incidence. Curves are collected at 105 K.

III. COMPUTATIONAL PROCEDURES

Theoretical $I(E)$ curves are calculated up to 260 eV with the LEED package of Van Hove and Tong.[11] After calculating reflection and transmission matrices within the self-consistent formalism, interlayer scattering is accomplished by layer doubling. Symmetry is used to reduce the computational effort. Up to 33 symmetry-nonequivalent beams are included when a twofold rotational axis and two orthogonal mirror planes are available as symmetry elements, which is the case when bulk layer registries are maintained throughout the crystal. Up to 61 symmetry-nonequivalent beams are included when only a mirror plane perpendicular to the $[1\bar{1}0]$ direction is available as a symmetry element, which is the case when the topmost layer is allowed to shift along the [001] direction. Two orientational domains must be considered when the topmost layer is allowed to shift (lateral displacements can be correlated in either the positive or negative [001] direction). Since the experimental LEED pattern contains a twofold rotational axis and two orthogonal mirror lines at normal incidence, the diffracted intensities from the two possible domains are assumed to add to the $I(E)$ curves with equal weight. To accomplish this theoretically, we first calculate the intensities for one domain and then sum the intensities of beams that are equivalent by symmetry when bulk layer registries are maintained throughout the crystal, but not equivalent by symmetry when the topmost layer is allowed to shift along the [001] direction.

Eight phase shifts ($l_{\max} = 7$) calculated from the tabulated, nonrelativistic Pd potential of Morruzi, Janak, and Williams[12] are used throughout. The phase shifts are corrected for temperature effects with an effective Debye temperature (θ_D) of 230 K. The real part of the optical potential (V_{or}) is assumed to be independent of energy, and is initially set at -10 eV. This parameter is treated as a variable during reliability-factor (r-factor) analysis, and is rigidly shifted in 1-eV steps to obtain the best level of agreement. The final value of V_{or} corresponding to the optimum geometry is -6 eV. The imaginary part of the optical potential (V_{oi}) is fixed at -4 eV. Optimization of θ_D and V_{oi} is not performed since the selected values are nearly identical to previously determined optimum values for Pd(110).[5]

Experimental and theoretical $I(E)$ curves are compared quantitatively with the Pendry r factor (r_P).[13] Since this r factor is highly sensitive to spectral noise,[13] both sets of curves are smoothed with two passes of a three-point smoothing algorithm[14] prior to r-factor analysis.

IV. RESULTS AND DISCUSSION

Varied structural parameters—the first interlayer spacing d_{12}, the second interlayer spacing d_{23}, and a registry shift of magnitude σ along the [001] direction in the topmost layer—are shown schematically in Fig. 2. We increment σ in steps of 0.1 Å, and for each value of σ we independently vary d_{12} and d_{23} over a wide range, both in steps of 0.025 Å. Since the proposed registry

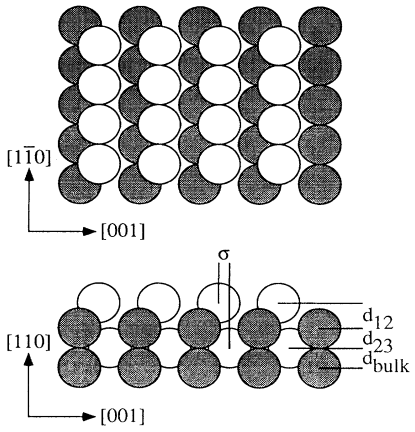

FIG. 2. Schematic of Pd(110) exhibiting a rigid registry shift along the [001] direction in the topmost layer.

shift is away from the hollow site and towards the short bridge site, increasingly larger values of d_{12} are tested for increasingly larger values of σ. In all cases, we allow d_{12} to range to values considerably larger than predicted by hard spheres of bulk metallic radius.

Figure 3 shows a representative comparison between experimental $I(E)$ curves and best-fit theoretical $I(E)$ curves for $\sigma=0$, 0.1, 0.2, and 0.7 Å. The displayed curves illustrate various degrees of response with respect to σ, with the (0,2) curve being the most sensitive and the (1,2) curve being the least sensitive. We find that $\sigma=0$, which corresponds to a nonlaterally displaced geometry, results in the lowest minimum r factor ($r_P=0.168$); however, our results do not conclusively rule out the presence of small lateral displacements. For example, the minimum r factor for $\sigma=0.1$ Å ($r_P=0.174$) is only negligibly higher than the value obtained for no lateral displacements. In order to determine the uncertainty in σ, we use Pendry's[13] definition of the variance $[\Delta r=r_{\min}(8V_{oi}/\Delta E)^{1/2}]$, which indicates that only geometries yielding $r_P>0.196$ can be ruled out as possible structures when one assumes that the minimum r factor obtained for $\sigma=0$ corresponds to the global minimum. The minimum r factor for $\sigma=0.2$ Å ($r_P=0.238$) clearly exceeds this value; thus, by interpolation, we estimate that the upper limit for σ is ca. 0.13 Å, which is considerably smaller than the value of 0.7 Å required to account for the He-atom diffraction results of Francis and Richardson. When σ is increased to 0.7 Å, the minimum r factor increases to an extremely poor value ($r_P=0.709$). As for the interlayer spacings, we find that $d_{12}=1.31\pm0.02$ Å and $d_{23}=1.39\pm0.02$ Å, which corresponds to a contraction of $(4.4\pm1.5)\%$ in d_{12} and an expansion of $(1.5\pm1.5)\%$ in d_{23} relative to the bulk interlayer spacing of 1.37 Å. Within the uncertainties, both d_{12} and d_{23} are found to be in agreement with the previously mentioned results of Diehl *et al.* and Skottke *et al.* Changes in deeper interlayer spacings are not studied since they are most likely smaller than their associated uncertainties.

The rather large uncertainty in σ can be attributed in part to momentum transfer being primarily normal to the surface in the normal-incidence configuration.[14] LEED's far greater sensitivity to vertical parameters at normal incidence is demonstrated by our results for $\sigma=0.2$ Å. Although $\sigma=0.2$ Å clearly exceeds the upper limit established in our analysis, optimum interlayer spacings for this value of σ differ by no more than 0.02 Å relative to those obtained for $\sigma=0$. While the use of the normal-incidence configuration surely diminishes LEED's sensitivity to lateral parameters, we find that domain averaging exerts an even larger effect. As shown in Fig. 4, theoretical $I(E)$ curves for the best-fit $\sigma=0.1$ Å geometry differ considerably from theoretical $I(E)$ curves for the optimum geometry prior to domain averaging, but only marginally after domain averaging.

Finally, we comment on the possible existence of an

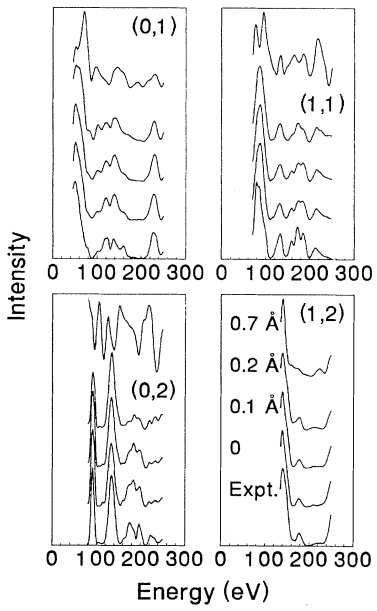

FIG. 3. Representative comparison between experimental $I(E)$ curves and best-fit theoretical $I(E)$ curves for $\sigma=0$, 0.1, 0.2, and 0.7 Å. Note the wide range of response with respect to σ.

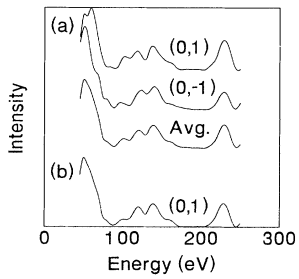

FIG. 4. (a) Theoretical $I(E)$ curves for the (0,1) and (0, −1) beams of a single orientational domain of the best-fit $\sigma=0.1$ Å geometry and their average. (b) Theoretical $I(E)$ curve for the (0,1) beam of the optimum geometry.

order-disorder transition on Pd(110) near 250 K. Although we cannot claim that we have reached a definitive conclusion concerning the absence or presence of lateral displacements, the fact that lateral displacements of the magnitude required to account for the He-atom diffraction results of Francis and Richardson are clearly not present indicates that if an order-disorder transition does exist, it is of a far more subtle nature. Since $I(E)$ curves collected above and below the proposed transition temperature do not differ significantly, we believe that the upper limit of ca. 0.13 Å for σ is also valid for a laterally disordered surface. As has been previously pointed out, the use of rigid registry shifts to model random lateral displacements is a good approximation due to the fact that the extent of intralayer multiple scattering is relatively small.[15]

ACKNOWLEDGMENTS

This work was supported by the National Science Foundation through Grant No. CHE-9014214. We thank R. J. Baird and G. W. Graham of Ford Motor Company for the use of their Pd(110) crystal. We also thank M. A. Van Hove for supplying the conventional LEED package, *r*-factor program, and phase shifts. One of us (O.L.W.) acknowledges the support of the Amoco Foundation. Another (P.A.T.) acknowledges support from the NSF Grant No. CHE-9024358, and from the Camille and Henry Dreyfus Foundation. Some equipment and all facilities are provided by the Ames Laboratory, which is operated for the U.S. Department of Energy by Iowa State University under Contract No. W-7405-ENG-82.

[1]S. M. Francis and N. V. Richardson, Phys. Rev. B **33**, 662 (1986).

[2]M. Wolf, A. Goschnick, J. Loboda-Cacković, M. Grunze, W. N. Unertl, and J. H. Block, Surf. Sci. **182**, 489 (1987).

[3]M. Guillopé and B. Legrand, Surf. Sci. **215**, 577 (1989).

[4]A. M. Lahee, J. P. Toennies, and Ch. Wöll, Surf. Sci. **191**, 529 (1987).

[5]R. D. Diehl, M. Lindroos, A. Kearsley, C. J. Barnes, and D. A. King, J. Phys. C **18**, 4069 (1985).

[6]M. Skottke, R. J. Behm, G. Ertl, V. Penka, and W. Moritz, J. Chem. Phys. **87**, 6191 (1987).

[7]R. Raval, S. Haq, M. A. Harrison, G. Blyholder, and D. A. King, Chem. Phys. Lett. **167**, 391 (1990).

[8]G. Kleinle, M. Skottke, V. Penka, G. Ertl, R. J. Behm, and W. Moritz, Surf. Sci. **189/190**, 177 (1987); H. Niehus, C. Hiller, and G. Comsa, *ibid.* **173**, L599 (1986).

[9]J. Goschnick, M. Wolf, M. Grunze, W. N. Unertl, J. H. Block, and J. Loboda-Cacković, Surf. Sci. **178**, 831 (1986).

[10]J. R. Noonan and H. L. Davis, in *Determination of Surface Structure by LEED,* edited by P. M. Marcus and F. Jona (Plenum, New York, 1984).

[11]M. A. Van Hove and S. Y. Tong, *Surface Crystallography by LEED* (Springer, Berlin, 1979).

[12]V. Moruzzi, J. Janak, and A. Williams, *Calculated Electronic Properties of Metals* (Pergamon, New York, 1978).

[13]J. B. Pendry, J. Phys. C **13**, 937 (1980).

[14]M. A. Van Hove, W. H. Weinberg, and C.-M. Chan, *Low-Energy Electron Diffraction* (Springer, Berlin, 1986).

[15]D. G. Kelly, R. F. Lin, M. A. Van Hove, and G. A. Somorjai, Surf. Sci. **224**, 97 (1989).